Development of Metallic Wear Debris Sensor Based on Eddy Current Technique

Sheng Chenxing [1,2*], Zhang Zongxin[1,2]
[1]Key Laboratory of Marine Power Engineering & Technology (Ministry of Transport)
Wuhan University of Technology
Wuhan, China
Email: scx01@126.com

Wang Huiyang[3]
[3]Wuhan united imaging healthcare Co. Ltd.
Wuhan, China

Han Yu[4]
[4]School of Mechanical Engineering,
Xi'an Jiaotong University
Xi'an,China

***Abstract*-On-line detection of metallic wear debris is an effective approach for condition monitoring of mechanical systems. Existing on-line oil conditioning sensors are mainly based on ferrography and inductive techniques. However, ferrography technique needs a clean background and inductive technique requires a high cleanliness of lubricant. To solve these issues, in this paper a metallic wear debris sensor based on eddy current principle is developed. Both numerical simulations and prototype experiments are conducted to evaluate the capacity and feasibility of the new sensor for detecting wear debris. The analysis results demonstrate that: 1) A pulse is generated when the wear debris pass through the sensor, the amplitude and width of the pulse can be used to identify the material and size of the debris; 2) The developed sensor is able to detect copper debris with a diameter greater than 150 μm and iron debris greater than 60 μm. This work provides a new idea for detecting wear debris and a new method for obtaining the characteristics of wear debris.**

Key words: metallic wear debris; eddy current; sensor

I. INTRODUCTION

Metallic wear debris is the most common and harmful pollutant in the lubrication system. It will cause second wear when flows through the friction surface due to its high hardness. What's worse, ferrous debris will be gathered under the action of the magnetic field, which will lead to the blockage of the orifice and gap. Beyond that, the metallic wear debris in lubricant is mainly the byproducts of friction wear, which contains a lot of information about the wear state of the mechanical equipment [1-3]. Therefore, on-line monitoring of metallic debris in oil plays an important role in oil monitoring and mechanical fault diagnosis [4-6].

At present, many types of researches have been carried out on the detection technologies about metallic wear debris, which mainly includes ferrography based on image processing and oil monitoring technique based on electromagnetic induction [7,8]. The size of wear debris can be recognized by the ferrography according to the color, and the size and the concentration of wear debris can also be recognized according to the proportion of wear debris. However, ferrography requires a clear view of the background and high quality picture, the darker color in lubricants and the overlap of wear debris can also result in a lower quality of picture [9]. Electromagnetic induction technique can judge the magnetic properties of wear debris by phase and recognize the size of wear debris by amplitude [10]. The most representative technology is the sensor designed by GasTOPS named MetalSCAN, where the ferromagnetic wear debris with a diameter of 100μm and the non-ferromagnetic wear debris with a diameter of 305μm can be recognized [11]. However, the sensor has three turns of coil, which results in a longer effective range of measurement. What's more, the sensor cannot effectively identify a large number of the continuous flow of wear debris in practical application, so it is always used for the detection for clean oil.

Since Michael Faradays discovered the electromagnetic induction and summed up the law of electromagnetic induction in 1831, the eddy current technology and its industrial applications have made great progress. Su [12] used eddy current technique to predict the size of a volumetric defect regardless of its location. Yu [13] used eddy current technique to measure the thickness of the material and coating layer. Kyungcho Kim used eddy current testing technique to detect loose parts in steam generators [14]. Perevertov [15] used eddy current technique to detect the modified surface at magnetizing frequencies from 0.2 to 10 kHz. Irazu and Elejabarrieta [16] discussed a contactless eddy current damper, which is used to attenuate structural vibration. Ulapane [17] proposed a ferromagnetic material thickness quantification method based on the Pulsed Eddy Current sensor. Eddy current technique can be used for detection of flaws, thickness variation and stress measurements in metallic materials [18-20]. Additionally, eddy current technique also can be used to attenuate structural vibration [21].

In this paper, the application of eddy current principle to metal wear debris detection is proposed. It is aimed to develop a sensor that is not affected by the color of the lubricating oil and the continuity of the wear debris. This sensor can also identify the material and size of the metallic wear debris. Through the simulation analysis of ANSYS Maxwell, it is theoretically proved that the eddy current technique is suitable for the detection of wear debris. On this

This work was supported by the NSFC-Zhejiang Joint Fund for the Integration of Industrialization and Informatization (Grant No. U1709215).

978-1-7281-0860-5/19/$31.00 ©2019 IEEE

basis, the effectiveness of the proposed method is proved by experimental study. This method provides a new idea to solve the problem that the common electromagnetic induction type wear debris sensor is susceptible to the continuity of the wear debris and the inability to identify the abrasive material.

This paper starts with the principle of eddy current testing, and combines the software of magnetic field simulation to simulate the sensor related parameters. Based on the simulation analysis, the sensor induction coil and signal processing circuit are designed, and the eddy current metal wear debris sensor is developed. Finally, the monitoring performance of the sensor is tested.

II. The Principle of Sensor Detection and Simulation Analysis of Sensor Parameters

A. The principle of sensor detection

According to Faraday law of electromagnetic induction, the metallic debris which is placed in a changing magnetic field will produce a vortex induced current when it cut magnetic lines in the magnetic field. This vortex induced current is called eddy current and the above phenomenon is called Eddy Current Effect. In this paper, the technique is applied to the detection of metallic wear debris, and its detection principle is shown in Figure 1. Both ends of the spiral coil are connected with the high-frequency alternating current named I1, the alternating magnetic field named H1 is generated in the metallic wear debris. When the metallic wear debris approaches the magnetic field, the wear debris in the circumferential direction can be equivalent to a circle of closed circuit, the magnetic flux in the closed circuit is constantly changing, so the eddy current is generated on the surface of the wear debris. At the same time, the eddy current field in the wear debris produces alternating magnetic field named H2, and the direction of H2 is opposite to that of H1, so that the voltage across the coil is reduced [22,23].

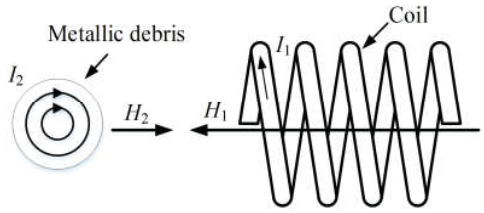

Figure 1 Principle diagram of sensor detection

The size of the eddy current produced by the metallic wear debris is affected by many factors, including the excitation frequency of the coil, the number of turns of the coil, the inner diameter of the coil, the size of the wear debris, and the material of the wear debris [23]. In order to study the effect of different parameters on the eddy current, ANSYS Maxwell is used to simulating the different parameters.

B. Simulation analysis

1) Model building

The length of the test coil (the number of turns of the coil) is short, so it can be simplified as a ring, and the metallic wear debris can be simplified as a spherical shape. The metallic wear debris is placed in the center of the coil, eddy current solver is used to calculate the model, as shown in Figure 2.

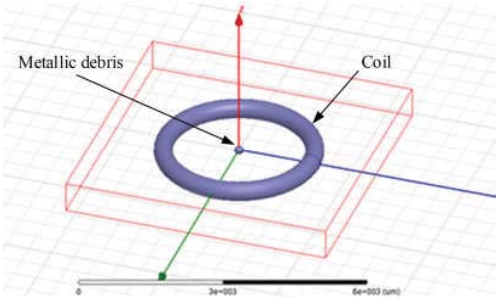

Figure 2 Maxwell 3D simulation model

2) Model correctness analysis

Figure 3 shows the eddy current density nephogram of 200μm copper wear debris at an excitation frequency of 10MHz and 1600μm internal diameter.

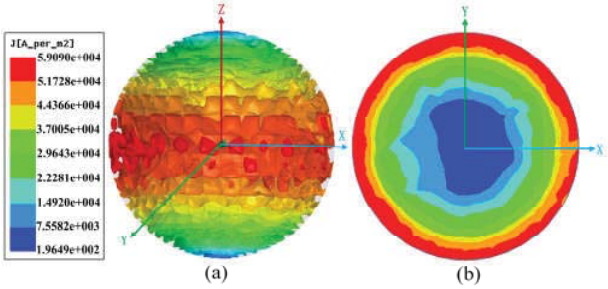

Figure 3 Eddy density nephogram of wear debris

It can be seen from Figure 3(a) that the eddy current density produced by the wear debris is stratified in the direction of the coil axis. The eddy current density is the largest at the center of the coil and gradually decreases toward both sides of the coil, which is consistent with the law of the magnetic flux density distribution of the coil.

It can be seen from Figure 3(b) that the eddy current density is unevenly distributed inside the wear debris and is the densest on the outer surface side of the wear debris. As the depth increases, the eddy current density gradually decays. This phenomenon is called skin effect [24,25]. In summary, the building model meets the objective physical laws and can represent the actual conditions.

Simulation analysis of different sensor parameters is shown as below, based on a function of ANSYS Maxwell named "Marker", 50 points were picked up at the center of the coil on the outer surface of the wear debris, and the average of the vortex density of the 50 points was used as a characteristic parameter to characterize the eddy current, and they were applied in the following simulation analysis.

3) Simulation analysis under different parameters

Considering the effect of the length of the sensor coil, the sensor is simplified as a ring, the turns of the coil is one, and the simulation results of the other parameters are shown in Figure 4.

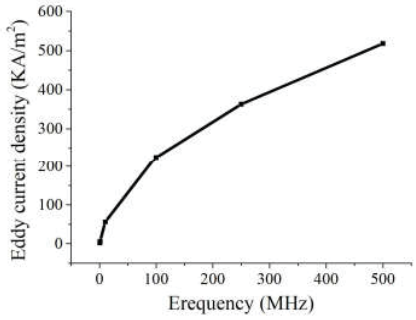

(a) Frequency - eddy current density

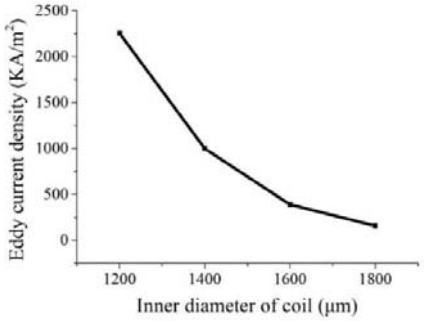

(b) Coil diameter - eddy current density

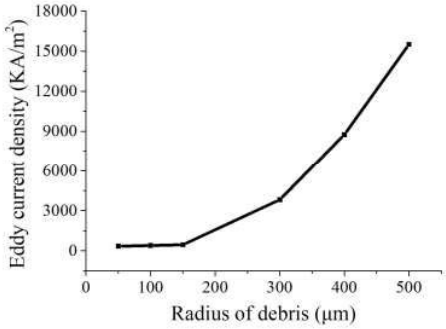

(c) Wear debris radius - eddy current density

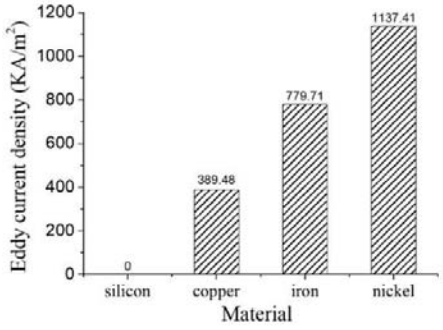

(d) Wear debris material - eddy current density

Figure 4 Simulation results of different parameters

Figure4(a) shows that the higher the excitation frequency is, the larger the eddy current density of the wear debris is, but the growth rate slows down as the frequency increases.

Figure4(b) shows that the larger the inner diameter of the coil is, the smaller the eddy current density of the wear debris is, and the eddy current slows down with the increase of the inner diameter.

Figure 4(c) shows that the relationship between the size of wear debris and the eddy current density is a non-linear monotonically increasing relationship. After the simulation data are fitted, the trend showed three power relationships. So the eddy current action can be used to identify the size of wear debris.

Figure4(d) shows that the eddy current density of the wear debris of different materials is different in the same magnetic field environment. Therefore, the eddy current technique can recognize the metallic wear debris: non-metallic wear debris (silicon) do not produce eddy currents, Wear debris have different electrical conductivity and permeability, the resulting eddy current density is also different.

III. Design of Sensors and Extraction of Wear debris Signals Features

A. design of test coil

According to the simulation results and experimental verification, the test coil design parameters are as follows.

1) The turns of coils: As shown in Figure2, the test coil can be designed as one turn which based on the eddy current testing technique. However , the output signal is easily interfered by unwanted signals such as noise and harmonics in the actual use of the sensor. In order to suppress unwanted signals in the output signal and improve the signal-to-noise ratio of the sensor. The number of turns is designed as three turns, according to several experimental results.

2) Excitation frequency: In order to increase the eddy current of wear debris and reduce the influence of magnetization on the detection of ferromagnetic wear debris, the excitation frequency of the coils should be increased as much as possible. However, excessive excitation frequency will cause the test signal to be interfered by high frequency noise signals. The excitation frequency cannot become large infinitely, and finally the excitation frequency is 280MHz.

3) The inner diameter of the coil: Figure4(b) shows that the smaller the inner diameter of the test coil is, the better the detection result is. However, with the diameter of the coil decreasing, the flow rate of the sensor will be limited, what's more, a small inner diameter of the coil increases the risk that the flow path is clogged by the larger wear debris, so the final diameter of the spiral pipe is 1.6mm.

B. Signal processing circuit design

In order to collect and output the electrical signals of wear debris effectively, the signal processing circuit of the sensor is designed, the principle of the signal processing circuit is shown in Figure 5. The DC voltage regulator circuit provides a stable DC power supply for the entire sensor, an alternating current oscillation circuit generates a high frequency in the test at both ends of the coil, when the metallic wear debris pass through the test coil, the test coil voltage will decrease, and the circuit will compensate for this part of the loss, after that, the noise signal is filtered by the low-pass filter circuit and then the amplified voltage is amplified by the amplifying circuit. Finally, the tiny voltage signal is amplified by the amplifier circuit and output.

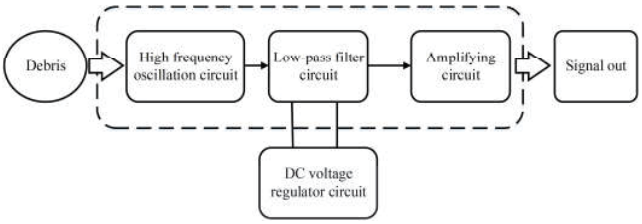

Figure 5 Schematic diagram of the signal processing circuit

C. Feature extraction of wear debris signals

Figure 6 shows that the pulse signal produced by iron debris with a diameter of 196 μm, the pulse amplitude (maximum voltage) contains information about the material and the size of wear debris, but the material and size of wear debris cannot be determined only by the pulse amplitude. In this context, the pulse width is constructed and it means the number of signal sampling points in the debris pulse signal that exceeds a certain threshold. This parameter indicates the time when the wear debris flows through the detection area of the induction coil. By analyzing the pulse amplitude and pulse width, the material and size of the wear debris can be identified. In order to eliminate the interference of the noise signal (Figure 7) when the pulse width is calculated, the pulse threshold of the pulse width should be slightly larger than the pulse amplitude (0.8V) of the noise signal. Finally, the threshold value is 1V.

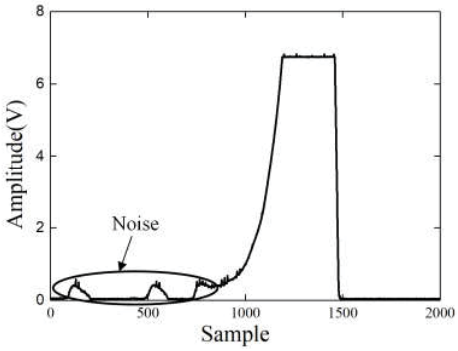

Figure 6 Pulse signal graph

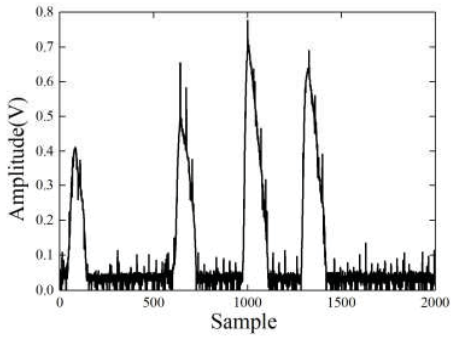

Figure 7 Noise signal graph

IV. SENSOR PERFORMANCE TEST

A. Test platform

The schematic diagram of the sensor test platform is shown in Figure 8, it mainly includes metallic wear debris sensor, power supply, stepping motor, sample, data acquisition card and data acquisition system.

The power supply provides 12V DC power for the wear debris sensor, stepper motor drives the sample at a certain speed (0.5m/s) through the test coil in the metallic wear debris sensor (The wheel and weights allow the sample to remain horizontal). The metallic wear debris sensor converts the coil disturbance into a voltage signal and acquires it via a data acquisition card (sampling frequency of 1 kHz). Finally, the test data is stored in the computer through a data storage system developed by LabVIEW.

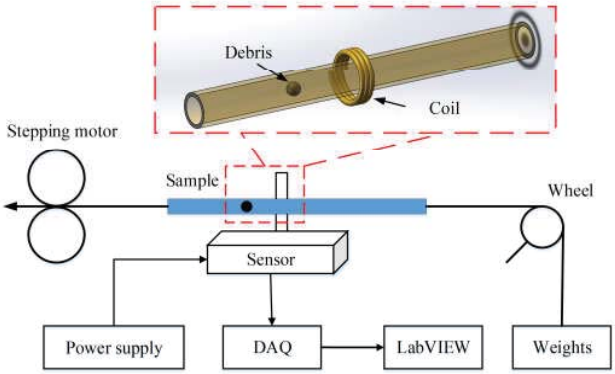

Figure 8 Schematic diagram of test platform

B. Wear debris test

1) Tests for wear debris of different sizes

Figure 9 shows the test results of wear debris in different sizes. From the test results of iron wear debris (Figure 9a), the minimum size of the copper wear debris which the sensor can effectively detect is 56 μm. Pulse amplitude and pulse width increase as the size of the iron wear debris increases. When the pulse amplitude increases to 6.8V, the amplification circuit enters the saturation working area, and the pulse amplitude does not increase.

From the test results of copper wear debris (Figure 9b), the minimum size of the copper wear debris which the sensor can effectively detect is 153 μm. As the copper wear debris size increases, the pulse amplitude will increase and the pulse width will also increase with the size of copper wear debris increases.

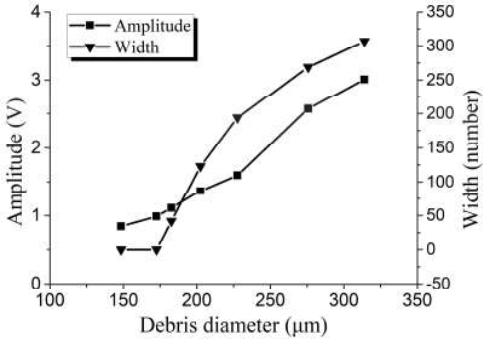

(a) Iron wear debris

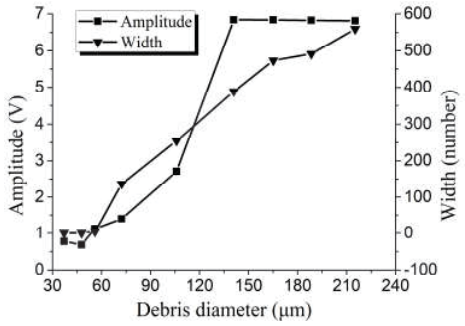

(b) Copper wear debris

Figure 9 Test results of wear debris of different sizes

2) Test on wear debris of different materials

Figure10 shows the experimental results of wear debris which have different material. As shown in Figure10(a), the pulse amplitude of the iron wear debris is greater than that of the copper wear debris. Figure10(b) shows the pulse width of the iron wear debris is greater than that of the copper wear debris which both have same size. The pulse amplitude of copper wear debris with a diameter of 150μm and 170μm is 0.9V, and it is greater than the pulse amplitude of the noise signal (0.8V), so it can be detected by the sensor. The pulse width is less than that of the measurement threshold, so the pulse width is 0.

Comparing the test results of different debris materials with the simulation results of different debris materials (Figure4d), the experimental data agrees with the simulation results. The eddy current action and sensor output of the iron wear debris are greater than the copper wear debris in the simulation analysis and test results.

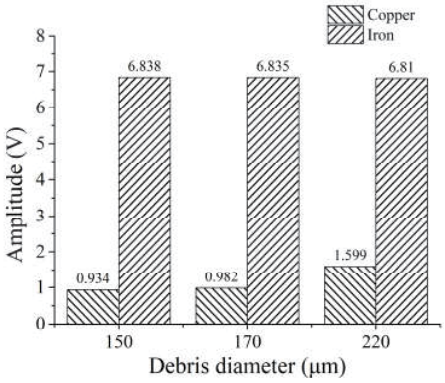

(a) Pulse amplitude

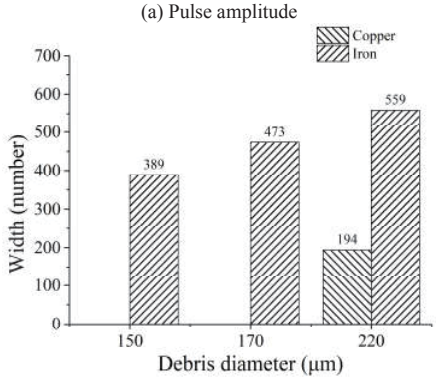

(b) Pulse width

Figure 10 Test results of wear debris of different materials

C. Application of wear debris detection

1) Detection for wear debris size

a) Iron wear debris

According to the pulse amplitude data of the iron wear debris, when the size of wear debris is less than 56μm, the sensor can not detect the effective wear debris signal, so the pulse amplitude is 0.8V which is the maximum value of the noise signal. When the size of wear debris is larger than 140μm, the amplification circuit in the signal processing enters the saturation working area, and the pulse amplitude is constant at 6.8V. When the size of the wear debris is 56~140μm, the test data is fitted by the polynomial of 3 times. The fitting process is shown in Figure11. The relationship between the size of the iron wear debris and the pulse amplitude is as follows.

$$\begin{cases} E = 0.8 & r < 56\mu m \\ E = 1.551 + 0.152r - 0.00149r^2 + 8.24e^{-6}r^3 & 56 \le r < 140\mu m \\ E = 6.8 & r \ge 140\mu m \end{cases} \quad (1)$$

In the Equation, E is the pulse amplitude and r is the wear debris size.

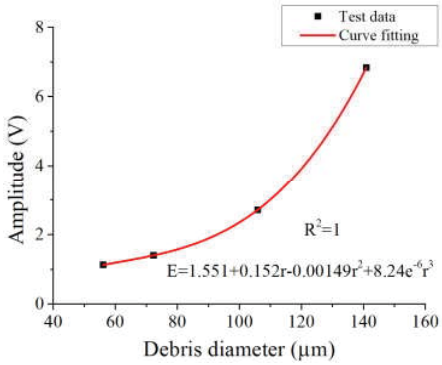

Figure 11 Fitting graph of iron wear debris amplitude data

Subsequent fitting of the pulse width data of the iron wear debris. Since the pulse width reflects the time when the wear debris flow through the induction coil, which is roughly linear with the size of the wear debris, the linear relationship is used to fit the pulse width. The fitting process is shown in Figure12, and the relationship between the size of the iron wear debris and the pulse width is obtained.

$$W = -125.485 + 3.37r \quad (2)$$

In the Equation, W is the pulse width and r is the size of the wear debris.

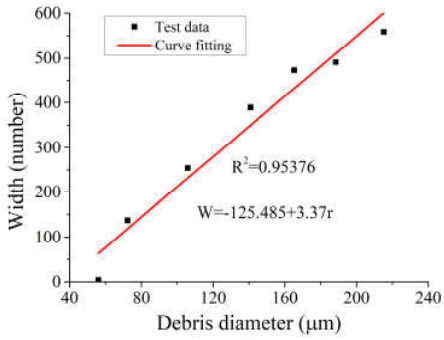

Figure 12 Fitting graph of iron wear grain pulse width data

When the iron wear debris size is unknown, the wear debris size can be identified by the pulse amplitude e1 of the measured signal and the pulse width w1 of the measured signal. If the measured pulse amplitude e1 is more than 6.8V, the measured pulse width w1 is taken into Eq.2 to determine the wear debris size r1. If the measured pulse amplitude e1 is less than 6.8V, since the data fit of the pulse amplitude is high, the pulse amplitude is used to judge the wear debris size. The measured pulse amplitude e1 is taken into Eq. 1 to determine the wear debris size r2, and the specific judgment flow is shown in Figure13.μm

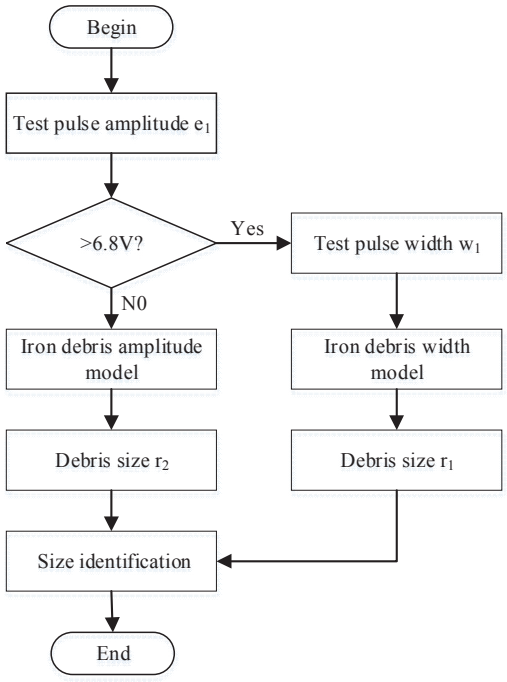

Figure 13 Flow chart for iron wear debris size identification

b) Copper wear debris

According to the data processing method of iron wear debris, to obtain the equations of copper wear grain size and pulse amplitude. The fitting process is shown in Figure14 and Figure15. Due to the limitations of the test conditions, the maximum copper wear grain obtained was 314 μm, and its pulse amplitude was 3 V, which did not reach the maximum value of 6.8 V of the sensor output. However, considering that the size of the copper wear debris exceeds 314 μm in practical applications, the equipment has undergone severe wear and it is meaningless to monitor its size. Therefore, when the wear grain size exceeds 314 μm, the output is recognized as 3V.

$$\begin{cases} E = 0.8 & r < 150\mu m \\ E = 11.634 - 0.156r + 7.145e^{-4}r^2 - 9.66e^{-6}r^3 & 150 \le r < 314\mu m \\ E = 3.0 & r \ge 314\mu m \end{cases} \quad (3)$$

In the Equation, E is the pulse amplitude and r is the wear debris size.

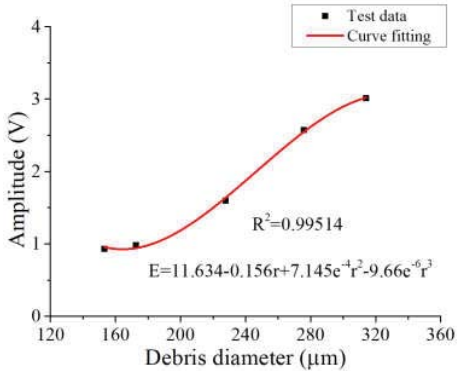

Figure 14 Fitting diagram of copper wear debris amplitude data

Subsequently, the pulse width data of the copper wear debris were fitted to obtain the relationship between the copper wear grain size and the pulse width:

$$W = -328.117 + 2.11r \quad (4)$$

In the Equation, W is the pulse width and r is the size of the wear debris.

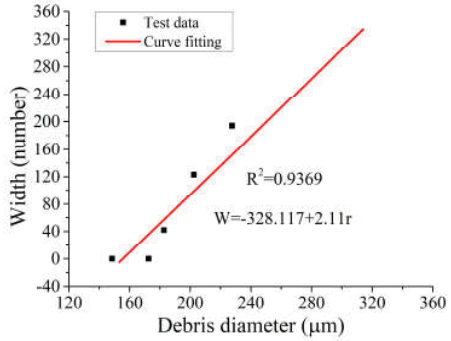

Figure 15 Fitting diagram of copper wear debris pulse width data

c) Detection for wear debris material and size

When the material and size of the wear debris are unknown, and the pulse amplitude e and the pulse width w are known, the iron wear debris size ri and the copper wear debris size rc corresponding to the pulse amplitude e are first solved by Eq. 1 and Eq. 3. Then ri, rc are respectively brought into Eq. 2and Eq. 4, the corresponding iron wear debris pulse width wi and copper wear debris pulse width wc are solved. Finally, w is compared with wi and wc. If w is equal to wi, it is judged to be iron wear debris of size ri. If w is approximately equal to wc, it is judged to be copper wear debris of size rc. If w is not equal to wi and wc, it is judged to be unknown wear debris, and the specific identification process is shown in Figure16.

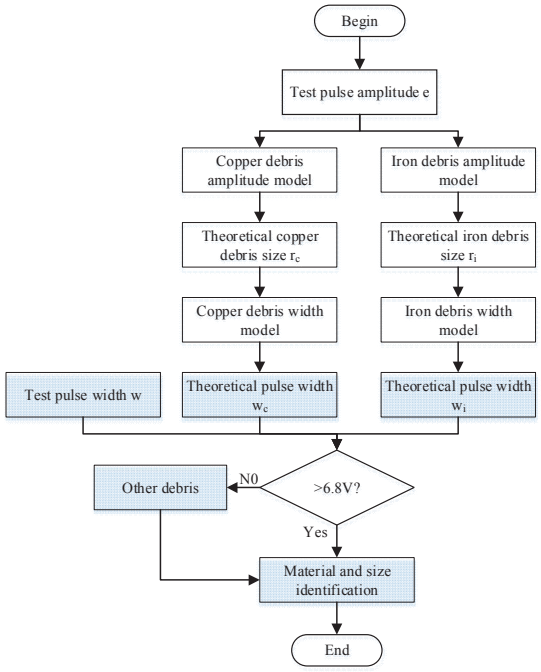

Figure 16 Flow chart for copper wear debris size identification

V. CONCLUSIONS

The detection of metallic wear debris in lubricating oil is of great significance to oil monitoring and fault diagnosis of mechanical equipment. In this paper, ANSYS Maxwell simulation software is used to simulate and analyze the parameters of the sensor. On this basis, the sensor test coil and signal processing circuit are designed. Finally, the sensor experimental rack is built and the experimental research is carried out. The conclusions of this paper are as follows:

1) According to ANSYS Maxwell simulation analysis, the relationship between the eddy current intensity and the size and the material of wear debris are obtained, the feasibility of eddy current technique for metallic wear debris detection is proved.

2) According to the technique of eddy current inspection, a new type of metallic wear debris detection sensor is designed. The sensor overcomes the limitations of the effect of the continuous wear debris and can work in heavily polluted oil paths. What's more, the size of the smallest copper wear debris which can be detected by this sensor is 150 μm, the size of the iron wear debris is 60 μm.

ACKNOWLEDGMENTS

The financial support of the present research was provided by the NSFC-Zhejiang Joint Fund for the Integration of Industrialization and Informatization (Grant No. U1709215).

REFERENCES

[1] J. Wang, J. Bi, L. Wang, and X. Wang, "A non-reference evaluation method for edge detection of wear particles in ferrograph images," Mech. Syst. Signal Process., vol. 100, pp. 863–876, 2018.

[2] W. Cao, G. Dong, Y.-B. Xie, and Z. Peng, "Prediction of wear trend of engines via on-line wear debris monitoring," Tribol. Int., vol. 120, pp. 510–519, 2018.

[3] Raadnui and Surapol, "Seal wear debris characterization for predictive maintenance," Wear, vol. 330–331, pp. 490–497, 2015.

[4] S. Feng, B. Fan, J. Mao, and Y. Xie, "Prediction on wear of a spur gearbox by on-line wear debris concentration monitoring," Wear, vol. 336–337, no. Switzerland, pp. 1–8, 2015.

[5] M. Henneberg, B. Jorgensen, and R. L. Eriksen, "Oil condition monitoring of gears onboard ships using a regression approach for multivariate T2 control charts," J. Process Control, vol. 46, pp. 1–10, 2016.

[6] T. Addabbo, A. Fort, R. Garbin, M. Mugnaini, S. Rocchi, and V. Vignoli, "Theoretical characterization of a gas path debris detection monitoring system based on electrostatic sensors and charge amplifiers," Measurement, vol. 64, pp. 138–146, 2015.

[7] T. H. Wu, H. K. Wu, Y. Du, and Z. X. Peng, "Progress and trend of sensor technology for on-line oil monitoring," Sci. China Technol. Sci., vol. 56, no. 12, pp. 2914–2926, 2013.

[8] H. Wei, W. Cai, S. Wang, and M. M. Tomovic, "Mechanical wear debris feature,detection,and diagnosis:A review," Chinese J. Aeronaut., vol. v.31;No.1, no. 5, pp. 5–20, 2018.

[9] Y. Peng, T. Wu, S. Wang, and Z. Peng, "Oxidation wear monitoring based on the color extraction of on-line wear debris," Wear, vol. 332–333, pp. 1151–1157, 2015.

[10] X. Zhu, C. Zhong, and J. Zhe, "Lubricating oil conditioning sensors for online machine health monitoring-A review," Tribol. Int., vol. 109, pp. 473–484, 2017.

[11] Gastops Long Live Equipment. MetalSCAN MS4000. (http://www.gastops.com/wp-content/uploads/2016/09/C008850_001.pdf) [accessed 20.12.16].

[12] Z. Su, L. Udpa, G. Giovinco, S. Ventre, and A. Tamburrino, "Monotonicity principle in pulsed eddy current testing and its application to defect sizing," in Applied Computational Electromagnetics Society Symposium-italy, 2017.

[13] Y. Yu, D. Zhang, C. Lai, and G. Tian, "Quantitative Approach for Thickness and Conductivity Measurement of Monolayer Coating by Dual-Frequency Eddy Current Technique," IEEE Trans. Instrum. Meas., vol. PP, no. 99, pp. 1–9, 2017.

[14] K. Kim, K. Min, C. Kim, J.-G. Kim, and M. Jhung, "Detectability evaluation of the loose parts in steam generator by eddy current testing techniques," Nucl. Eng. Technol., vol. 50, no. 7, pp. 1160–1167, 2018.

[15] [1] O. Perevertov, M. Neslušan, and A. Stupakov, "Detection of milled 100Cr6 steel surface by eddy current and incremental permeance methods," Ndt E Int., vol. 87, no. Complete, pp. 15–23, 2017.

[16] L. Irazu and M. J. Elejabarrieta, "Analysis and numerical modelling of eddy current damper for vibration problems," J. Sound Vib., vol. 426, pp. 75–89, 2018.

[17] N. Ulapane, A. Alempijevic, J. V. Miro, and T. Vidal-Calleja, "Non-destructive evaluation of ferromagnetic material thickness using Pulsed Eddy Current sensor detector coil voltage decay rate," NDT E Int., vol. 100, pp. 108–114, 2018.

[18] K. S. Rao, S. Mahadevan, B. P. C. Rao, and S. Thirunavukkarasu, "A new approach to increase the subsurface flaw detection capability of pulsed eddy current technique," Measurement, vol. 128, pp. 516–526, 2018.

[19] A. Habibalahi and M. S. Safizadeh, "Pulsed eddy current and ultrasonic data fusion applied to stress measurement," Meas. Sci. Technol., vol. 25, no. 5, pp. 1009–1016, 2014.

[20] M. Fan, B. Cao, A. I. Sunny, W. Li, G. Tian, and B. Ye, "Pulsed eddy current thickness measurement using phase features immune to liftoff effect," Ndt E Int., vol. 86, no. Complete, pp. 123–131, 2017.

[21] L. Irazu and M. J. Elejabarrieta, "Analysis and numerical modelling of eddy current damper for vibration problems," J. Sound Vib., vol. 426, pp. 75–89, 2018.

[22] Y. B. He, W. W. Feng, and K. Jiang, "Finite Element Analysis on Multi Parameter Characteristics of Inductive Lubricating Oil Wear Debris Sensor," Appl. Mech. Mater., vol. 738–739, pp. 97–102, 2015.

[23] K. Haldar and D. C. Lagoudas, "Dynamic magnetic shape memory alloys responses: Eddy current effect and Joule heating," J. Magn. Magn. Mater., vol. 465, pp. 278–289, 2018.

[24] Y. Yu, P. Du, and Y. Liao, "Study on effect of coil shape and geometric parameters on performance of eddy current sensor," Chinese J. Sci. Instrum., vol. 28, no. 6, pp. 1045–1050, 2007.

[25] J. Szeftel, N. Sandeau, and A. Khater, “Study of the skin effect in superconducting materials,” Phys. Lett. A, vol. 381, no. 17, pp. 1525–1528, 2017.

[26] S. Jiao, X. Liu, and Z. Zeng, “Intensive Study of Skin Effect in Eddy Current Testing with Pancake Coil,” IEEE Trans. Magn., vol. 53, no. 7, pp. 1–8, 2017.

[27] S. Hamada, F. Z. Louai, N. Nait-Said, and A. Benabou, “Dynamic hysteresis modeling including skin effect using diffusion equation model,” J. Magn. Magn. Mater., vol. 410, pp. 137–143, 2016.